Homepage Journal http://jurnal.polsri.ac.id/index.php/austenit

AUSTENIT VOL. 15 NO.2, OKTOBER 2023 ISSN : 2085-1286 E-ISSN : 2622-7649

BIOCOMPATIBLE P(TM co SA-CAA) HYDROGELS WITH pH RESPONSIVE AND ENHANCED MECHANICAL PERFORMANCE

Gustini[1)]*, Kaprawi[1)], Hasan Basri[1)], Irmawan[2)], Irsyadi Yani[1)], Nurhabibah Paramita Eka Utami[1)]

[1)] Mechanical Engineering, Sriwijaya University, Jl.Raya Palembang-Prabumulih KM. 32 Inderalaya Ogan Ilir OI South Sumatera

[2)] Electrical Engineering, Sriwijaya University, Jl.Raya Palembang-Prabumulih KM. 32 Inderalaya Ogan Ilir OI South Sumatera

*Corresponding email: gustini@unsri.ac.id

ARTICLE INFORMATION

Revised
12/09/2023

Accepted
18/09/2023

Online Publication
31/10/2023

©2023 The Authors. Published by AUSTENIT (Indexed in SINTA)

doi:

doi.org/10.5281/zenodo.10060585

ABSTRACT

In recent years, development of hydrogel that combines biocompatibility, pH responsive and mechanical performance has attracted the attention of researchers. A novel biocompatible hydrogel, composed of P(TM co SA) and P(TM co CAA) was synthesized by a simple admixture and heating process. The results show that with increasing levels of SA-CAA monomer concentration, an increase in tensile strength and elongation at breakpoint was observed and optimal at the ratios P(TM co SA CAA). Tensile strength and young's modulus registered an impressive increase of 43% and 40% respectively. These improvements are attributed to strong synergistic hydrogen bonding interactions between the TM and SA-CAA chains. During the experiment, maximum increase in weight was also achieved at pH 10 NaOH solution, it is show the pH-responsive hydrogels. The investigation of P(TM co SA-CAA) hydrogel mechanism showed that more homogenous dispersed through crosslinks dominated by β-sheets from Amide I structures. Furthermore, the SA-CAA molecules contributed to the biocompatibility, pH responsive and mechanical performance of P(TM co SA-CAA) hydrogels. Conclusively, its P(TM co SA-CAA) hydrogels clearly demonstrated the relevance of the provide a bio-responsive material for biomedical applications, such as tissue engineering, regenerative medicine and pH-sensitive drug delivery.

Keywords *: Biocompatible, P(TM co SA-CAA) Hydrogels, Mechanical Performance, pH Responsive*

1 INTRODUCTION

Hydrogels are a type of soft nature, hydrated form and synthetic elastomeric materials (Gao et al., 2015; Jankaew et al., 2015; Seliktar, 2012; Xiang et al., 2017), which have broad applications in biomedical fields (Annabi et al., 2014; Censi, Di Martino, Vermonden, & Hennink, 2012; Guilak, Butler, Goldstein, & Baaijens, 2014; H. Li et al., 2015; Y. Li & Kumacheva, 2018; Sun et al., 2013; Yue, Haque, Kurokawa, Nakajima, & Gong, 2013). The most frequently investigated scaffolds come from the Polyethylene glycol (PEG) group of molecules, polyethylene glycol hydrogels use as a tissue engineering (Lin & Anseth, 2009; Lubich et al., 2016; Tagami, Uehara, Moriyoshi, Ishida, & Kiwada, 2011). However, a shortcoming of polyethylene glycol (PEG) is the vulnerability of polyethylene glycol to oxidation, which inhibits proliferation use in tissue engineering applications (Hershfield et al., 2014; Tagami et al., 2011). The fact that chemical added ingredient must be used to incorporate bioactive functional family into polyethylene glycol hydrogels. Finally, there are increasing witnesses that some humans have begun to produce antibodies against polyethylene glycol, which shows that it cannot function as a universal tissue engineering platform (Barcellona, Johnson, & Bernards, 2015; Cao, Barcellona, Pfeiffer, & Bernards, 2016; Erathodiyil, Chan, Wu, & Ying, 2020; Hershfield et al., 2014; Lubich et al., 2016; Schroeder, Zurick, McGrath, & Bernards, 2013; Tagami et al., 2011). Accordingly, substitute chemistries are selected for tissue engineering applications. The zwitterionic functional group has been the main alternative to replace polyethylene glycol (Barcellona et al., 2015; Erathodiyil et al., 2020). Other group members who are related to the zwitterionic material group is the polyampholite hydrogels, which are consisted of mixing cationic and anionic charged monomer subunits. (Blackman, Gunatillake, Cass, & Locock, 2019;

Colilla, Izquierdo-Barba, & Vallet-Regí, 2018; Jain, Matsumura, & C, 2016; Schroeder et al., 2013; Tao et al., 2018).

Zwitterionic pH responsive hydrogels have acid–alkaline groups. Its pH responsive comes from the ionization of two groups in the hydrogel network. A pH responsive hydrogel is a polymer hydrogel that can change in volume with changes in the environmental pH. Generally, pH responsive hydrogels can be divided into three different response types, which are anionic, cationic, and zwitterionic. Its molecular structure usually has an amino group. (C.-P. Li, Weng, & Huang, 2020; Takahashi, Lira, & de Torresi, 2012).

Polyampholyte hydrogels represent amorphous in structure for biomedical materials applications as polyampholyte hydrogels have some similar features to those of glassy polymers that can bind the covalent bonds of bioactive molecules without needing a change of their base chemistry (Haag & Bernards, 2020; Schroeder et al., 2013; Tah, Bernards, & Biointerfaces, 2012). The physical behaviour of polyampholyte hydrogels relies on their cationic and anionic charged ionic monomer subunits despite similar hydrogel synthesis procedures (Cao et al., 2016; Dobbins, McGrath, & Bernards, 2012; Schroeder et al., 2013; Sun et al., 2013; Tah et al., 2012). Moreover, It has been known that the molecular chain architecture and mechanical performance of hydrogels can be improved by the intrinsic stiffly of the polymeric chains, crosslinking density and varying monomers concentration (Costa & Mano, 2015; Luong, Browning, Bixler, & Cosgriff-Hernandez, 2014; Xiang et al., 2017). In this study, the biocompatibility, pH responsive and mechanical performance of P(TM-co SA-CAA) hydrogels under various anionic monomer ratios were investigated. The P(TM co SA-CAA) hydrogels are constructed by two copolymerizations including cationic and anionic charged ionic monomer subunits. The ionic bonds consist of strong bonds and weak bonds which play key role for mechanical properties of the hydrogels. Young's modulus and elongation at break ability can be tuned over a wide range by choosing the proper cationic and anionic ions combination. The strong bonds attend as steady crosslinks to preserve the shape and primary network of the hydrogels, whereas the weak bonds toughen the sacrificial network of the materials. We used the strong bonds and weak bonds of each ionic monomers, with strong bonds composing of cationic [2(methacryloyloxy) ethyl] trimethyl-ammonium chloride (TM) and another strong (3 Sulfopropyl methacrylate potassium salt (SA) and weak (2 Carboxyethyl acrylate (CAA) bonds is a compound that consists anionic based on the five ratios. Here, sodium hydroxide solvent can be used to reduce the cytotoxic effects of P(TM-co SA-CAA). The impact of anionic monomer ratios on the biocompatibility, pH responsive and mechanical performance was assessed. It increases the choices of synthetic polyampholyte hydrogels with combinations of biocompatibility, pH responsive and mechanical performance, and the simple polymerization process is easy to scale up for mass production. It is hypothesized that P(TM-co SA-CAA) hydrogels exhibited biocompatibility, pH responsive materials and enhanced mechanical properties, which is promising for use as materials in the biomedical field such as a tissue engineering applications, regenerative medicine and pH-sensitive drug delivery.

2. MATERIALS AND METHODS

2.1 Materials

[2(methacryloyloxy)ethyl] trimethylammo-nium chloride (TM), 3 Sulfopropyl methacrylate potassium salt (SA), 2 Carboxyethyl acrylate (CAA), triethylene glycol dimethacrylate (TEGDMA) were purchased from Sigma Aldrich (St. Louis, MO). Ethylene glycol, sodium hydroxide (NaOH), ammonium persulfate (APS), sodium metabisulfite (SMS), Phosphate buffered saline (PBS; 150 mM, pH 7.4) and Milk Q water, fetal bovine serum (FBS), trypsin ethylene-diaminetetraacetic acid, penicillin streptomycin, were used directly without further purification The cell MC3T3-E1 it was purchased from ATCC. All chemicals were used as received. Which is shown in Figure 1.

2.2. Preparation of P(TM co SA-CAA) hydrogels

P(TM co SA-CAA) hydrogels were synthesized 2.0 mmol of total monomer and the volume of TEGDMA, using the molar ratio of each monomer, with 1.0 mmol composed of cationic monomer TM and another 1.0 mmol is a compounding of anionic monomer SA and CAA based on the five ratios under research. A solution of NaOH, ethylene glycol and ethanol was mixed in a 1.5:1.5:1 ratio and, preparations were adjusted from before with slight changes. (Cao et al., 2016; Dobbins et al., 2012). Briefly, The P(TM co SA-CAA) hydrogels with different anionic monomer molar ratios were referred to as P(TM co SA), P(TM co CAA) and P(TM co SA- CAA), The polymerization was started using 80 µL of a 40% APS solution and 80 µL of a 15% SMS in Milk Q water. The solution was well mixed and put in polytetrafluoroethylene spacer with a thickness of 1 mm, which is located between two glass microscope slides. The reaction worked at 60 ˚C for 1 hour which is shown on Fig.1, and then the

gel was cooled at room temperature for 1 hour before the investigation was carried out. Before being used for further research, all hydrogels were soaked in PBS for 24 hours.

Blank 1 space Arial 10

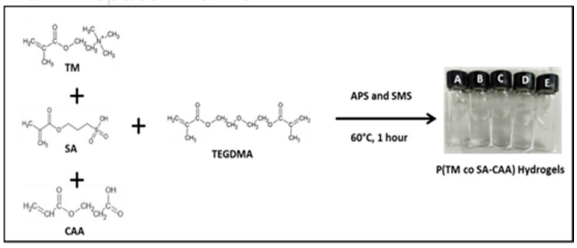

Figure 1. Schematics of production P(TM co SA-CAA) Hydrogel

2.3. Evaluation of pH responsivity

The hydrogel was removed from the mould, after hydrogel synthesis, and then trimmed into 10 mm disks. The disks were put in a 24 well plate with 1 mL of NaOH solution [25]. This neutral PH of NaOH solution was selected to preserve local pH balance around to the surface of the hydrogel. To prevent evaporation, all well plates were plated cover, and measurements of the PH of the samples were taken once every day for seven days. After pH measurements were taken, all samples were immersed with fresh NaOH solution each day. Moreover, the pH responsivity of the hydrogels can be calculated using standard test method for NaOH solution absorption of polymer (ASTM D570) was measurements in different pH numbers, ranging from 3 to 10 NaOH solution. The increase in weight of the hydrogels can be calculated using eq. (1).

$$\boldsymbol{Q_{eq}}, \% = \frac{wet\ weight - conditioned\ weight}{conditioned\ weight} x100 \qquad (1)$$

$\boldsymbol{Q_{eq}}$ is equilibrium NaOH solution absorption calculated the as grams of NaOH solution per gram of the gel sample. All the measurements were repeated at least five times to extract the average values. Based on the environmental pH results, the equilibrium of various P(TM co SA-CAA) hydrogels after immersed for two days. The equilibrium NaOH solution absorption was measurements by the rate of the swollen disks surface area because the disks surface area dimensions of the hydrogel are significantly larger than the thickness of the hydrogel (Costa & Mano, 2015; Wong, Akaishi, Longaker, & Gurtner, 2011).

2.4. Mechanical test

The mechanical properties of P(TM co SA-CAA) hydrogels tests were taken at room temperature. P(TM co SA-CAA) hydrogels with various SA-CAA contents were determined using a FGP-0.5 Nidec-SHIMPO. For measurement, the uniaxial tensile tests, samples with 1 mm thickness bars shapes were prepared to adhere to the ISO 37 Type 3. Measurement conditions for the tensile test were as follows: the tensile speed was 20 mm•min-1. The initial cross-sectional area of 10 mm2 was used to calculate the stress and strain tensile. The tensile stress, young's modulus and elongation at break were calculated to evaluate their tensile mechanical performance thoroughly. Sample measurements were repeated five times to acquire the average values.

2.5. Evaluation of the cytotoxicity

A Standard of the ISO 10993-5(1999) "Biological evaluation of medical devices-Part 5: Tests for in vitro cytotoxicity" is used to evaluate Cytotoxicity test of P(TM co SA-CAA) hydrogels. The sample preparation was a synthesis with different anionic monomer molar ratios were referred to as P(TM co SA), P(TM co CAA) and P(TM co SA-CAA), The hydrogel disks with a diameter of 10 mm were individually placed into a 24-well plate and then soaked into sterile PBS buffer for one day for sterility. The nutrient medium used was DMEM 90v/v%, 1v/v% penicillin-streptomycin and 10v/v% FBS. The preparation of cell culture was as follows: MC3T3-E1 cells were incubated which was supplemented with DMEM 90v/v%, 1v/v% penicillin-streptomycin and 10v/v% FBS in a humidified atmosphere at 37□C and 5% CO2. To proliferate, the cells were washed twice with 3 mL of PBS liquid and the nutrient medium was changed every two days. The cells are ready for use after seven days of incubation and can be used for experiments. After incubation, P (TM co SA-CAA) hydrogels were transferred to 24 well plates sterile and seeding on the hydrogels surface used MC3T3-E1 mouse. Seeding using 1.0 × 104 cells for Cell adhesion on P(TM co SA-CAA) hydrogels and each well containing were 90v/v% DMEM, 1v/v% penicillin-streptomycin and 10v/v% FBS. Using a 3 mL PBS buffer, the cells were washed twice and then 2 ml of trypsin was added to separate the cells. The cells were counted using a hemocytometer. 1 mL of cell solution and nutrient medium were added on P (TM co SA-CAA) hydrogels surfaces each well and then was placed in an incubator for 24 hours. After that, samples were stained and imaged and then for the proliferation time (for one day to seven days), samples was reverted to the incubator and was stained and imaged. All the images were repeated at least five randomly located for each sample.

3. RESULTS AND DISCUSSION

3.1 Secondary Structure in proteins of P(TM co SA) and P(TM co CAA) in P(TM co SA-CAA) hydrogels.

The fact that mechanical performance of TM co SA-CAA exhibit great differences compared to hydrogel P(TM co SA) and P(TM co CAA) inspired us to further investigate the secondary structure of P(TM co SA) and P(TM co CAA) in the P(TM co SA-CAA) hydrogels as well as investigating the effect of adding SA and CAA during the polymerization process. Admixtures P(TM co CAA) and P(TM co SA) in the P(TM co SA-CAA) hydrogels were collected to characteristics of SA and CAA molecules when polymerization process. All these P(TM co SA) and P(TM co CAA) based hydrogels were dominated are β-sheet from amide I structures pivotal for the crosslinking of the P(TM co SA-CAA) hydrogels network. Based on research results (Censi et al., 2012), the amide I peaks around between 1600 and 1700 cm^{-1} is associated with β-sheet conformations of SA-CAA, respectively.

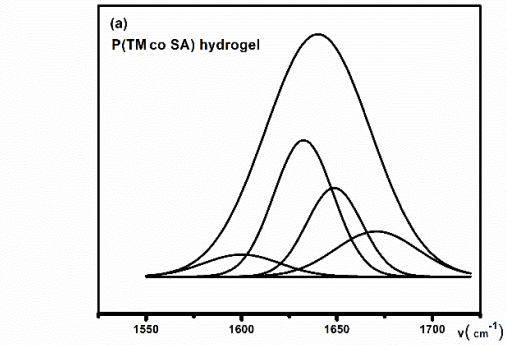

Figure 2. Amide I band decomposition using Gaussian components for P(TM co SA) hydrogels

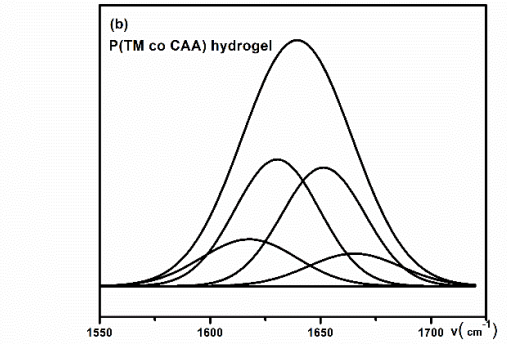

Figure 3. Amide I band decomposition using Gaussian components for P(TM co CAA) hydrogels.

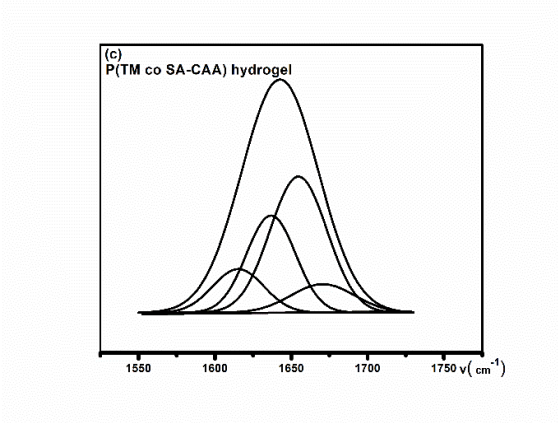

Figure 4. Amide I band decomposition using Gaussian components for P(TM co SA-CAA)

Table 1. Peaks of secondary structures deconvolution amide I and content (in %) of P(TM co SA), P(TM co CAA) and P(TM co SA-CAA) hydrogels.

P(TM co SA)		P(TM co CAA)		P(TM co SA-CAA)	
β-sheet (cm^{-1})		β-sheet (cm^{-1})		β-sheet (cm^{-1})	
v, (cm^{-1})	Ø, %	v, (cm^{-1})	Ø, %	v, (cm^{-1})	Ø, %
1633	25.4	1641	44.3	1655	11.5
1650	19.4	1658	18.4	1636	11.8
1674	22.9	1619	29.0	1615	16.8
1601	5.5	1680	16.3	1672	30.0

Amide I protein is the band most sensitive to secondary structure changes (Barth, 2007; Kong & Yu, 2007). The secondary structure of P(TM co SA) and P(TM co CAA) showed that amide I band resolved into five component peaks which are clearly seen on Fig.2, Fig.3 and P(TM co SA-CAA) hydrogels secondary structure showed amide I band was resolved into five component peaks which is shown on Fig. 4. The peaks shown are β-sheet of secondary structures based on average wavenumbers. The amide I band decomposition using five Gaussian components, result are peaks of secondary structures deconvolution amide I and content (in %) of P(TM co SA) and P(TM co CAA) hydrogels (Fig. 2 and Fig.3) and P(TM co SA-CAA) hydrogels (Fig. 4). The peaks percentages for of P(TM co SA), P(TM co CAA) and P(TM co SA-CAA) hydrogels are shown in Table 1. β-sheet molecular structure of SA and CAA molecules serving as the crosslinking and diffusing equally in P(TM co SA-CAA) hydrogel, which was the effect the vital cause for the enhancing mechanical performance of P(TM co SA-CAA) hydrogels.

3.2. pH-responsivity of P(TM co SA-CAA) hydrogels.

The effect of environmental pH on P(TM co SA-CAA) hydrogels was investigated at room temperature for seven days, and using NaOH solution checked a pH meter (LAQUA F-71S by Horiba). The result is shown in Fig. 5. Each hydrogel sample was immersed in NaOH solution to observe the release of ions into the NaOH solution, and the accumulation of pH on the samples surface because of the vital role this surface area plays in the toxicity of the P(TM co SA-CAA) hydrogels. After two days of immersing, the environmental pH reached equilibrium (pH-7) for all of P(TM co SA-CAA) hydrogels, as shown in Fig. 5. It is due to the protonation of the amino groups excessive of ions, which are present in the monomer subunits.

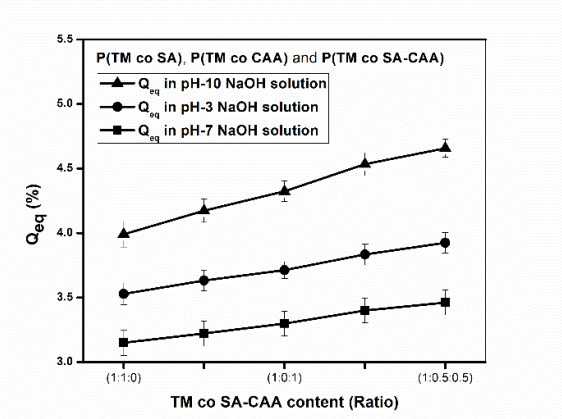

Figure 5. Ion release of P(TM co SA-CAA) hydrogels, which composited of different mixture ratios, at different pH values ranging forms (3,7 and 10).

The Increase in weight per cent of five groups of the P(TM co SA-CAA) hydrogel samples were characterized in the NaOH solutions which were turned the pH values ranging from 3,7 and 10, and the results of the Increase in weight per cent responsive versus pH values were presented in Fig. 5. Five samples of the P(TM co SA-CAA) hydrogel samples were composited of the TM and SA-CAA monomers, which contain cationic and anionic functional groups, respectively. The mixture ratio of the TM remained as 1.0 mmol, and another 1.0 mmol is a compounding of SA and CAA based on the five ratios in three groups were separately added following with the ratios of the 1:0, 0:1 and 0.5:0.5. The pH value on the hydrogel swelling ratio P (TM co SA-CAA) was affected by the basis of protonation of the amino groups of TM. In the alkaline pH, the protonation of the amide groups leads to repulsion in the cationic chains is increased, thus allowing more NaOH solution in the hydrogel network. At acidic pH, deprotonation of the amide groups takes place, and repulsion in amide chains is reduced. This results in the shrinking of the hydrogels and therefore, the amount of NaOH solution in the hydrogel decreases. Below acidic pH, TM as cationic at the amide groups converted to carboxyl groups. However, into alkaline conditions at pH=10, the anionic character of hydrogel predominates. As a result, ionic pressure within hydrogels is increased relative to the solution media and hydrogels achieve equilibrium through Increase in weight. Finally, the increased in weight percent at pH values can be attributed to the conversion of non-ionic carboxylic acid pendants to anionic carboxylate groups. (Philippova, Barabanova, Molchanov, & Khokhlov, 2011; Su & Okay, 2017).

3.3. Mechanical performance of P(TM co SA-CAA) hydrogels.

In this experiment, a series of P(TM co SA-CAA) hydrogels with variations TM co SA, TM co CAA and TM co SA-CAA, monomers SA-CAA were studied, where monomer ratio has a significant influence on the P(TM co SA-CAA) hydrogels behaviour. Fig.6 showed the mechanical behaviour representative stress–strain curves of the P(TM co SA-CAA) hydrogels with different mixing ratios of P(TM co SA) and P(TM co CAA) where P(TM co SA) and P(TM co CAA) shows the tensile strength of 0.88 and 1.26 MPa. Mechanical behaviour P(TM co SA) hydrogel was highly low, and it can be fractured easily during the tensile test. In contrast, a simultaneous increase in hydrogel tensile strength with the addition of CAA monomers and maximum on P(TM co SA-CAA) hydrogels were observed. This is by previous studies which reported the best monomer ratio in a Polyampholyte hydrogel is a balanced ratio of 1:1, cations and anions.(Haag & Bernards, 2020). Additionally, the excellent mechanical strength is gradually enhanced are also revealed by the tensile stress–strain curves of the P(TM co SA-CAA) hydrogels. It is noted that impressive 73% and 70% improvement in the tensile strength (from 0.88 to 1.26 MPa) and young's modulus (from 0.80 to 1.18 MPa), respectively, could be achieved with SA-CAA addition, which are equivalent to or better than those of the P(TM co SA) hydrogels or P(TM co CAA) hydrogels.(Cao et al., 2016; Dobbins et al., 2012; Mariner, Haag, & Bernards, 2019; Schroeder et al., 2013).

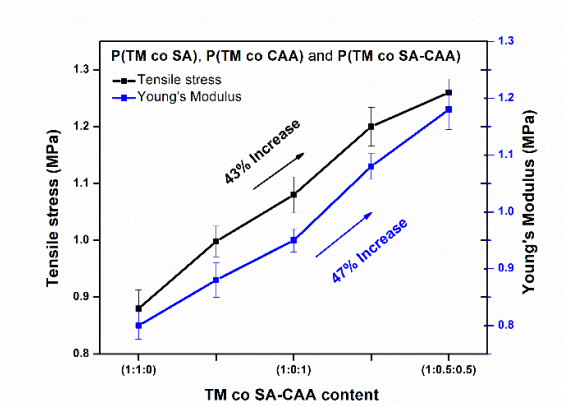

Figure 6. Mechanical performance of P(TM co SA-CAA) hydrogels. Highly tensile properties of composite hydrogels with an increasing SA-CAA content are controlledly enhanced.

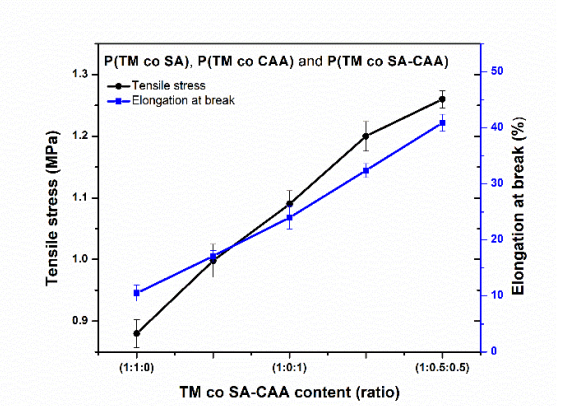

Figure 7. Mechanical performance of P(TM co SA-CAA) hydrogels. Highly tensile stress of P(TM co SA-CAA) hydrogels with an increasing SA-CAA content.

Improvements of up to 43, and 43 % in tensile and Young's modulus and elongation at break can be achieved with (1:0.5:0.5) ratio SA-CAA added. The identical case was as well evaluated at the elongation at break of the P(TM co SA-CAA) hydrogels. The P(TM co SA-CAA) hydrogels which result in the maximum young's modulus and elongation was P(TM co SA-CAA) hydrogels. It is beneficial to state that we used TEDGMA as a crosslinker for the P(TM co SA-CAA) hydrogels which also contributes towards tensile strength such as young's modulus and elongation because of the result the optimum alignment of pendant side chains from adjoining hydrocarbons polymer chains. Consequently, there is the realignment of the water interconnection and crosslinker, where is a significantly increased elastic modulus (slope) (Mariner et al., 2019). The synergistic hydrocarbons polymer chains interactions and hydrogen bonding may precisely lead to smaller and more uniform β-sheet structure. β-sheet structure as the crosslinking and dispersed evenly in the hydrogel network, which was attributed to the vital reason for the superior mechanical performance of P(TM co SA-CAA) hydrogels.

3.4. Biocompatibility evaluation of P(TM co SA-CAA) hydrogels.

It is well known that cells contain many biomolecules, such as proteins and nucleic acids [42] and cells have the capability to taste and react to the stiffness of their surroundings (Discher, Janmey, & Wang, 2005). Cell activities such as adhesion, migration, cytokinesis, morphogenesis, and proliferation are controlled by regulating the stiffness of the matrix. The dynamic forces such as tensile strength were able to an increase in cell viability and proliferation as compared to static forces. Therefore, the regeneration of proteins was an increase in the high tensile strength group (Discher et al., 2005). Based on these, five ratio hydrogels with different monomer were evaluated for their biocompatibility as a cells scaffold for P(TM co SA-CAA) hydrogels. Here, MC3T3-E1 cells were seeded onto the P(TM co SA-CAA) hydrogels and the cell survival using FDA staining assay after seven days of cell culture. The identification of the number of live and intact cells still embedded in the hydrogels surface used FDA staining. The cells count was determined as the number of live cells over the total number of counted cells per mm^2 of hydrogels. Fig. 8 showed the representative microscopy images for all P(TM co SA-CAA) hydrogels with different monomers ratios. After day-1 of adhesion, all the P(TM co SA-CAA) hydrogels showed no toxic and all monomers ratio had adherent cells with good viability. Overall, cells within P(TM co SA-CAA) hydrogels showed the increased live cells rate after seven days. Based on the tensile measurements, P(TM co SA-CAA) hydrogels ratio showed the highest stiffness, and higher initial cells live. The cells live All P(TM co SA-CAA) hydrogels have a statistically significant increase in the number of cells at day-7 (Fig. 8) higher than the results from P(TMA co CAA) surfaces (Lubich et al., 2016). This result indicates that all of P(TM co SA-CAA) hydrogels monomer ratio are non-toxic, but most importantly, this all of monomers ratio maintains high cell live and viability and long-term cytotoxicity.

3.5. Biocompatibility evaluation of P(TM co SA-CAA) hydrogels.

It is well known that cells contain many biomolecules, such as proteins and nucleic acids (Alberts et al., 2002) and cells have the capability to taste and react to the stiffness of their surroundings (Discher et al., 2005). Cell activities

such as adhesion, migration, cytokinesis, morphogenesis, and proliferation are controlled by regulating the stiffness of the matrix. The dynamic forces such as tensile strength were able to an increase in cell viability and proliferation as compared to static forces. Therefore, the regeneration of proteins was an increase in the high tensile strength group (Discher et al., 2005). Based on these, five ratio hydrogels with different monomer were evaluated for their biocompatibility as a cells scaffold for P(TM co SA-CAA) hydrogels. Here, MC3T3-E1 cells were seeded onto the P(TM co SA-CAA) hydrogels and the cell survival using FDA staining assay after seven days of cell culture. The identification of the number of live and intact cells still embedded in the hydrogels surface used FDA staining. The cells count was determined as the number of live cells over the total number of counted cells per mm^2 of hydrogels. Fig. 8 showed the representative microscopy images for all P(TM co SA-CAA) hydrogels with different monomers ratios. After day-1 of adhesion, all the P(TM co SA-CAA) hydrogels showed no toxic and all monomers ratio had adherent cells with good viability. Overall, cells within P(TM co SA-CAA) hydrogels showed the increased live cells rate after seven days. Based on the tensile measurements, P(TM co SA-CAA) hydrogels ratio showed the highest stiffness, and higher initial cells live. The cells live All P(TM co SA-CAA) hydrogels have a statistically significant increase in the number of cells at day-7 (Fig. 8) higher than the results from P(TMA co CAA) surfaces (Schroeder et al., 2013). This result indicates that all of P(TM co SA-CAA) hydrogels monomer ratio are non-toxic, but most importantly, this all of monomers ratio maintains high cell live and viability and long-term cytotoxicity.

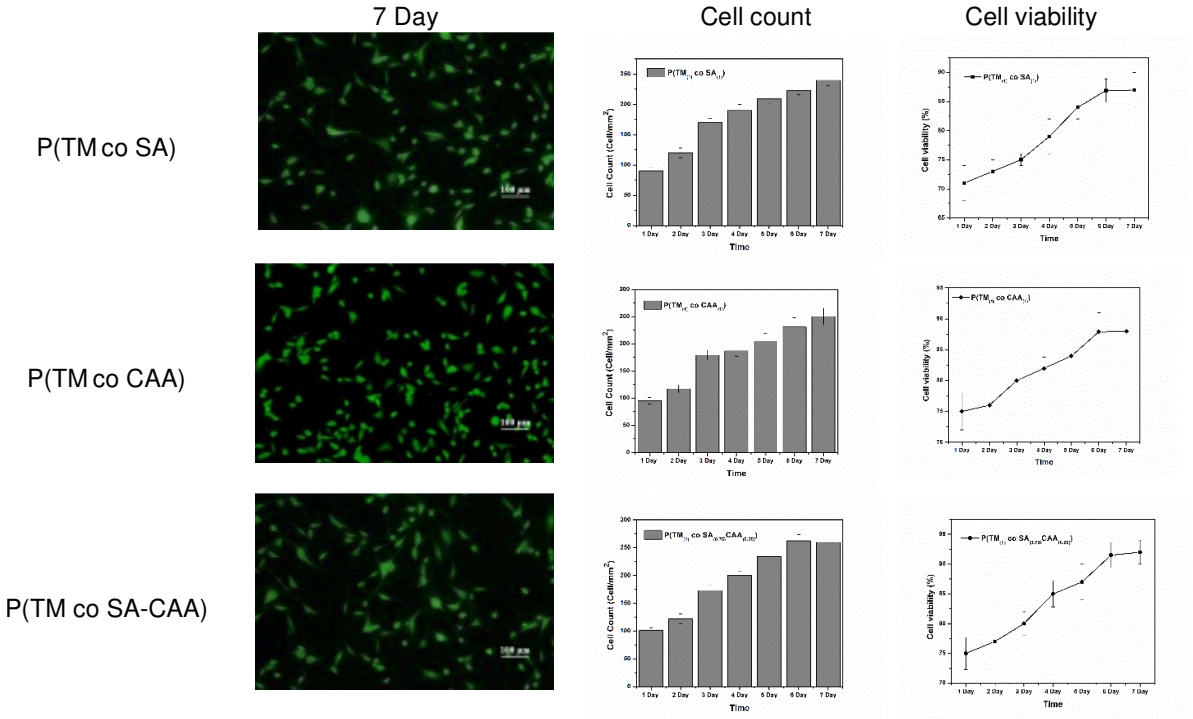

Figure 8. Representative fluorescent microscopy images of MC3T3–E1 cultured, scale bar = 100 µm, cell count assay and cell viability assay of P(TM co SA-CAA) hydrogels.

After showing the cell live of P(TM co SA-CAA) hydrogels, we proceeded to cell count assay and cell viability assay to further validate the performance of the P(TM co SA-CAA) hydrogels. Fig. 8 showed representative microscopy images for all P(TM co SA-CAA) hydrogels and quantitative analysis. Overall, the P(TM co SA-CAA) hydrogels showed a good initial cell adhesion due to their high conjugation rate that results from the increasing concentration of counterions during hydrogel synthesis and these hydrogels sustained a high viability cell population over seven days of cell culture. Finally, biocompatibility of P(TM co SA-CAA) hydrogels demonstrate their promising applications as hydrogel materials for tissue engineering applications.

4. CONCLUSION

In this work, we combined the P(TM co SA) and P(TM co CAA) with a biocompatible, pH-responsive and mechanical performance by

admixture then heating. These results indicated that the FTIR spectrum shows the formation of electrostatic interactions involving the positively charged TM group and the negatively charged SA-CAA group which has a synergistic effect dominated by small β sheet structure even homogeneously dispersed and enhanced mechanical performance. It is caused by the impact of conformational ordering on amide (β-sheet) electrostatic complexation. The increase in weight per cent at alkaline pH values can be attributed to converting non-ionic carboxylic acid pendants to anionic carboxylate groups. Cytotoxicity in vitro of P(TM co SA-CAA) hydrogels was further studied using cell adhesion and proliferation that promoted high cell viability. P(TM co SA-CAA) hydrogels showed high cell viability and good biocompatibility. Therefore, the P(TM co SA-CAA) hydrogels can be promising as hydrogel materials for biomedical applications, such as alternative templates for tissue regeneration, regenerative medicine and drug delivery.

REFERENCES

Alberts, B., Johnson, A., Lewis, J., Raff, M., Roberts, K., & Walter, P. (2002). Cell movements and the shaping of the vertebrate body. In *Molecular Biology of the Cell. 4th edition*: Garland Science. https://www.ncbi.nlm.nih.gov/books/NBK21054/

Annabi, N., Tamayol, A., Uquillas, J. A., Akbari, M., Bertassoni, L. E., Cha, C., . . . Khademhosseini, A. J. A. m. (2014). 25th anniversary article: Rational design and applications of hydrogels in regenerative medicine. *26*(1), 85-124. https://doi.org/10.1002/adma.201303233

Barcellona, M. N., Johnson, N., & Bernards, M. T. J. L. (2015). Characterizing drug release from nonfouling polyampholyte hydrogels. *31*(49), 13402-13409. https://doi.org/10.1021/acs.langmuir.5b03597

Barth, A. J. B. e. B. A.-B. (2007). Infrared spectroscopy of proteins. *1767*(9), 1073-1101. https://doi.org/10.1007/s11340-021-00741-6

Blackman, L. D., Gunatillake, P. A., Cass, P., & Locock, K. E. J. C. S. R. (2019). An introduction to zwitterionic polymer behavior and applications in solution and at surfaces. *48*(3), 757-770. https://doi.org/10.1039/C8CS00508G

Cao, S., Barcellona, M. N., Pfeiffer, F., & Bernards, M. T. J. J. o. A. P. S. (2016). Tunable multifunctional tissue engineering scaffolds composed of three-component polyampholyte polymers. *133*(40). https://doi.org/10.1002/app.43985

Censi, R., Di Martino, P., Vermonden, T., & Hennink, W. E. J. J. o. C. R. (2012). Hydrogels for protein delivery in tissue engineering. *161*(2),680-692. https://doi.org/10.1016/j.jconrel.2012.03.002

Colilla, M., Izquierdo-Barba, I., & Vallet-Regí, M. J. M. (2018). The role of zwitterionic materials in the fight against proteins and bacteria. *5*(4), 125. https://doi.org/10.3390/medicines5040125

Costa, A. M., & Mano, J. F. J. E. P. J. (2015). Extremely strong and tough hydrogels as prospective candidates for tissue repair–A review.*72*,344-364. https://doi.org/10.1016/j.eurpolymj.2015.07.053

Discher, D. E., Janmey, P., & Wang, Y.-l. J. S. (2005). Tissue cells feel and respond to the stiffness of their substrate. *310*(5751), 1139-1143. DOI: 10.1126/science.1116995

Dobbins, S. C., McGrath, D. E., & Bernards, M. T. J. T. J. o. P. C. B. (2012). Nonfouling hydrogels formed from charged monomer subunits. *116*(49),14346-14352. https://doi.org/10.1021/jp307588b

Erathodiyil, N., Chan, H.-M., Wu, H., & Ying, J. Y. J. M. T. (2020). Zwitterionic polymers and hydrogels for antibiofouling applications in implan table devices. *38*, 84-98. https://doi.org/10.1016/j.mattod.2020.03.024

Gao, X., Shi, Z., Liu, C., Yang, G., Sevostianov, I., & Silberschmidt, V. V. J. P. T. (2015). Inelastic behaviour of bacterial cellulose hydrogel: In aqua cyclic tests. *44*, 82-92. https://doi.org/10.1016/j.polymertesting.2015.03.021

Guilak, F., Butler, D. L., Goldstein, S. A., & Baaijens, F. P. J. J. o. b. (2014). Biomechanics and mechanobiology in functional tissue engineering. *47*(9), 1933-1940. https://doi.org/10.1016/j.jbiomech.2014.04.019

Haag, S. L., & Bernards, M. T. J. L. (2020). Enhanced biocompatibility of polyampholyte hydrogels. *36*(13), 3292-3299. https://doi.org/10.1021/acs.langmuir.0c00114

Hershfield, M. S., Ganson, N. J., Kelly, S. J., Scarlett, E. L., Jaggers, D. A., Sundy, J. S. J. A. r., & therapy. (2014). Induced and pre-existing anti-polyethylene glycol antibody in a trial of every 3-week dosing of pegloticase for refractory gout, including in organ transplant recipients.*16*(2),1-11. https://doi.org/10.1186/ar4500

Jain, M., Matsumura, K. J. M. S., & C, E. (2016). Thixotropic injectable hydrogel using a polyampholyte and nanosilicate prepared directly after cryopreservation. *69*, 1273-1281. https://doi.org/10.1016/j.jhazmat.2010.06.098

Jankaew, R., Rodkate, N., Lamlertthon, S., Rutnakornpituk, B., Wichai, U., Ross, G., & Rutnakornpituk, M. J. P. T. (2015). “Smart” carboxymethylchitosan hydrogels crosslinked with poly (N-isopropylacrylamide) and poly (acrylic acid) for controlled drug release. *42*,

26-36. https://doi.org/10.1016/j.polymertesting.2014.12.010

Kong, J., & Yu, S. J. A. b. e. b. S. (2007). Fourier transform infrared spectroscopic analysis of protein secondary structures. *39*(8), 549-559. https://doi.org/10.1111/j.1745-7270.2007.00320.x

Li, C.-P., Weng, M.-C., & Huang, S.-L. J. P. (2020). Preparation and characterization of pH sensitive Chitosan/3-Glycidyloxypropyl Trimethoxysilane (GPTMS) hydrogels by sol-gel method. *12*(6), 1326. DOI: 10.3390/polym12061326

Li, H., Wu, R., Zhu, J., Guo, P., Ren, W., Xu, S., & Wang, J. J. J. o. P. S. P. B. P. P. (2015). pH/temperature double responsive behaviors and mechanical strength of laponite-crosslinked poly (DEA-co-DMAEMA) nanocomposite hydrogels. *53*(12), 876-884. https://doi.org/10.1002/polb.23713

Li, Y., & Kumacheva, E. J. S. a. (2018). Hydrogel microenvironments for cancer spheroid growth and drug screening. *4*(4), eaas8998. https://doi.org/10.1002/polb.23713

Lin, C.-C., & Anseth, K. S. J. P. r. (2009). PEG hydrogels for the controlled release of biomolecules in regenerative medicine. *26*, 631-643. DOI: 10.1126/sciadv.aas8998

Lubich, C., Allacher, P., de la Rosa, M., Bauer, A., Prenninger, T., Horling, F. M., . . . Reipert, B. M. J. P. r. (2016). The mystery of antibodies against polyethylene glycol (PEG)-what do we know? , *33*, 2239-2249. https://doi.org/10.1007/s11095-016-1961-x

Luong, P., Browning, M., Bixler, R., & Cosgriff-Hernandez, E. J. J. o. B. M. R. P. A. (2014). Drying and storage effects on poly (ethylene glycol) hydrogel mechanical properties and bioactivity. *102*(9), 3066-3076. doi: 10.1002/jbm.a.34977

Mariner, E., Haag, S. L., & Bernards, M. T. J. B. (2019). Impacts of cross-linker chain length on the physical properties of polyampholyte hydrogels. *14*(3). https://doi.org/10.1116/1.5097412

Philippova, O., Barabanova, A., Molchanov, V., & Khokhlov, A. J. E. p. j. (2011). Magnetic polymer beads: Recent trends and developments in synthetic design and applications. *47*(4), 542-559. https://doi.org/10.1016/j.eurpolymj.2010.11.006

Schroeder, M. E., Zurick, K. M., McGrath, D. E., & Bernards, M. T. J. B. (2013). Multifunctional polyampholyte hydrogels with fouling resistance and protein conjugation capacity. *14*(9), 3112-3122. https://doi.org/10.1021/bm4007369

Seliktar, D. J. S. (2012). Designing cell-compatible hydrogels for biomedical applications. *336*(6085), 1124-1128. DOI: 10.1126/science.1214804

Su, E., & Okay, O. J. E. P. J. (2017). Polyampholyte hydrogels formed via electrostatic and hydrophobic interactions. *88*, 191-204. https://doi.org/10.1016/j.eurpolymj.2017.01.029

Sun, T. L., Kurokawa, T., Kuroda, S., Ihsan, A. B., Akasaki, T., Sato, K., Gong, J. P. J. N. m. (2013). Physical hydrogels composed of polyampholytes demonstrate high toughness and viscoelasticity. *12*(10), 932-937. DOI: 10.1038/nmat3713

Tagami, T., Uehara, Y., Moriyoshi, N., Ishida, T., & Kiwada, H. J. J. o. C. R. (2011). Anti-PEG IgM production by siRNA encapsulated in a PEGylated lipid nanocarrier is dependent on the sequence of the siRNA. *151*(2), 149-154. https://doi.org/10.1016/j.jconrel.2010.12.013

Tah, T., Bernards, M. T. J. C., & Biointerfaces, S. B. (2012). Nonfouling polyampholyte polymer brushes with protein conjugation capacity. *93*, 195-201. https://doi.org/10.1016/j.colsurfb.2012.01.004

Takahashi, S. H., Lira, L. M., & de Torresi, S. I. C. (2012). Zero-order release profiles from a multistimuli responsive electro-conductive hydrogel. DOI:10.4236/jbnb.2012.322032

Tao, Y., Wang, S., Zhang, X., Wang, Z., Tao, Y., & Wang, X. J. B. (2018). Synthesis and properties of alternating polypeptoids and polyampholytes as protein-resistant polymers. *19*(3), 936-942. https://doi.org/10.1021/acs.biomac.7b01719

Wong, V. W., Akaishi, S., Longaker, M. T., & Gurtner, G. C. J. J. o. I. D. (2011). Pushing back: wound mechanotransduction in repair and regeneration. *131*(11), 2186-2196. https://doi.org/10.1038/jid.2011.212

Xiang, H., Xia, M., Cunningham, A., Chen, W., Sun, B., & Zhu, M. J. J. o. t. M. B. o. B. M. (2017). Mechanical properties of biocompatible clay/P (MEO2MA-co-OEGMA) nanocomposite hydrogels. *72*, 74-81. https://doi.org/10.1016/j.jmbbm.2017.04.026

Yue, Y. F., Haque, M. A., Kurokawa, T., Nakajima, T., & Gong, J. P. J. A. m. (2013). Lamellar hydrogels with high toughness and ternary tunable photonic stop-band. *25*(22), 3106-3110. https://doi.org/10.1002/adma.201300775.